JPn Neuroscience
The Journal of Physiology

J Physiol 594.13 (2016) pp 3609–3628

Phospholipase C δ4 regulates cold sensitivity in mice

Yevgen Yudin[1], Brianna Lutz[2], Yuan-Xiang Tao[1,2] and Tibor Rohacs[1]

[1] *Department of Pharmacology, Physiology and Neuroscience, Rutgers, New Jersey Medical School, Newark, NJ, USA*
[2] *Department of Anesthesiology, Rutgers, New Jersey Medical School, Newark, NJ, USA*

Key points

- The cold- and menthol-activated transient receptor potential melastatin 8 (TRPM8) channels are thought to be regulated by phospholipase C (PLC), but neither the specific PLC isoform nor the *in vivo* relevance of this regulation has been established.
- Here we identify PLCδ4 as the key PLC isoform involved in regulation of TRPM8 channels *in vivo*.
- We show that in small PLCδ4$^{-/-}$ TRPM8-positive dorsal root ganglion neurons cold, menthol and WS-12, a selective TRPM8 agonist, evoked significantly larger currents than in wild-type neurons, and action potential frequencies induced by menthol or by current injections were also higher in PLCδ4$^{-/-}$ neurons.
- PLCδ4$^{-/-}$ mice showed increased behavioural responses to evaporative cooling, and this effect was inhibited by a TRPM8 antagonist; behavioural responses to heat and mechanical stimuli were not altered.
- We provide evidence for the involvement of a specific PLC isoform in the regulation of cold sensitivity in mice by regulating TRPM8 activity.

Abstract The transient receptor potential melastatin 8 (TRPM8) ion channel is a major sensor of environmental low temperatures. Ca^{2+}-induced activation of phospholipase C (PLC) has been implied in the regulation of TRPM8 channels during menthol- and cold-induced desensitization *in vitro*. Here we identify PLCδ4 as the key PLC isoform involved in regulation of TRPM8 in sensory dorsal root ganglion (DRG) neurons. We identified two TRPM8-positive neuronal subpopulations, based on their cell body size. Most TRPM8-positive small neurons also responded to capsaicin, and had significantly larger menthol-induced inward current densities than medium–large cells, most of which did not respond to capsaicin. Small, but not medium–large, PLCδ4$^{-/-}$ neurons showed significantly larger currents induced by cold, menthol or WS-12, a specific TRPM8 agonist, compared to wild-type (WT) neurons, but TRPM8 protein levels were not different between the two groups. In current-clamp experiments small neurons had more depolarized resting membrane potentials, and required smaller current injections to generate action potentials (APs) than medium–large cells. In small PLCδ4$^{-/-}$ neurons, menthol application induced larger depolarizations and generation of APs with frequencies significantly higher compared to WT neurons. In behavioural experiments PLCδ4$^{-/-}$ mice showed greater sensitivity to evaporative cooling by acetone than control animals. Pretreatment with the TRPM8 antagonist PBMC reduced cold-induced responses, and the effect was more pronounced in the PLCδ4$^{-/-}$ group. Heat and mechanical sensitivity of the PLCδ4$^{-/-}$ mice was not different from WT animals. Our data support the involvement of PLCδ4 in the regulation of TRPM8 channel activity *in vivo*.

(Resubmitted 22 February 2016; accepted after revision 5 April 2016; first published online 8 April 2016)
Corresponding author T. Rohacs: Department of Pharmacology, Physiology and Neuroscience, Rutgers, New Jersey Medical School, 185 South Orange Ave., MSB H631, Newark, NJ 07103, USA. Email: rohacsti@njms.rutgers.edu

DOI: 10.1113/JP272321

Abbreviations AP, action potential; DRG, dorsal root ganglion; GFP, green fluorescent protein; GPCR, G-protein coupled receptor; DMEM, Dulbecco's modified Eagle's medium; HBSS, Hank's buffered salt solution; PBMC, (*S*)-1-phenylethyl(2-aminoethyl)(4-(benzyloxy)-3 methoxybenzyl)carbamate; $PI(4,5)P_2$, phosphatidylinositol 4,5-bisphosphate; PLC, phospholipase C; TRPA1, transient receptor potential ankyrin 1; TRPM8, transient receptor potential melastatin 8; TRPV1, transient receptor potential vanilloid 1; WS-12, (1*R**,2*S**)-*N*-(4-methoxyphenyl)-5-methyl-2-(1 methylethyl)cyclohexanecarboxamide.

Introduction

Transient receptor potential melastatin 8 (TRPM8) ion channels are expressed in sensory neurons of the dorsal root ganglia (DRG) and trigeminal ganglia (TG), and they are activated by cold, menthol and other chemical agonists such as such as icilin and WS-12 ((1*R**,2*S**)-*N*-(4-methoxyphenyl)-5-methyl-2-(1 methylethyl)cyclohexanecarboxamide) (McKemy *et al.* 2002; Peier *et al.* 2002). $TRPM8^{-/-}$ mice have significantly reduced sensitivity to moderate cold, showing that these channels are major sensors of environmental low temperatures (Bautista *et al.* 2007; Colburn *et al.* 2007; Dhaka *et al.* 2007).

The activity of TRPM8 channels depends on the presence of the membrane phospholipid phosphatidylinositol 4,5-bisphosphate [$PI(4,5)P_2$] (Rohacs, 2014). TRPM8 currents run down in excised patches, and application of $PI(4,5)P_2$ reactivates the channel (Liu & Qin, 2005; Rohacs *et al.* 2005). TRPM8 was shown to be inhibited in intact cells by chemically inducible 5-phosphatases (Varnai *et al.* 2006; Daniels *et al.* 2009) and a voltage inducible 5′-phosphatase (Yudin *et al.* 2011), both of which deplete $PI(4,5)P_2$ without generating any second messengers. The purified TRPM8 protein incorporated into planar lipid bilayers required $PI(4,5)P_2$ for both cold and menthol activation (Zakharian *et al.* 2010), showing that the lipid acts directly on the channel. $PI(4,5)P_2$ was also shown to be important for setting the temperature threshold for TRPM8 (Fujita *et al.* 2013).

When TRPM8 channels are continuously stimulated by menthol or cold, their activity decreases over time in the presence of extracellular Ca^{2+} (McKemy *et al.* 2002), a phenomenon termed desensitization, or adaption (reviewed by Yudin & Rohacs, 2011). Based mainly on experiments in heterologous expression systems, it was shown that desensitization is caused by activation of a Ca^{2+}-sensitive phospholipase C (PLC) enzyme, and the consequential decrease of $PI(4,5)P_2$ (Rohacs *et al.* 2005; Daniels *et al.* 2009; Yudin *et al.* 2011). Cold adaptation in mice was shown to be reduced by PLC inhibitors, but the PLC isoform involved in this phenomenon was not identified (Brenner *et al.* 2014). Also, the currently available PLC inhibitors are quite non-specific, and have many side effects (Balla, 2001), including weak stimulation of PLC (Horowitz *et al.* 2005), and thus we set out to study the role of PLC using a genetic approach. The most abundant highly Ca^{2+}-sensitive PLC isoform in DRG neurons is PLCδ4 (Daniels *et al.* 2009; Lukacs *et al.* 2013; Thakur *et al.* 2014), and mRNA for this enzyme was shown to be enriched in TRPM8-positive DRG neurons (Knowlton *et al.* 2013).

To assess the role of PLCδ4 in regulation of TRPM8, we tested sensitivity of DRG neurons from $PLC\delta4^{-/-}$ mice to cold and chemical TRPM8 agonists. Our data show that both the TRPM8 agonists menthol and WS-12, and cold induced larger current responses in small TRPM8-positive DRG neurons isolated from $PLC\delta4^{-/-}$ mice, compared to small WT neurons. Medium and larger TRPM8-positive neurons had lower current densities than small neurons, and currents in these cells were not different between $PLC\delta4^{-/-}$ and wild-type (WT). In current clamp measurements menthol induced action potentials (APs) with higher frequencies in small neurons isolated from $PLC\delta4^{-/-}$ animals compared to cells from WT mice. In behavioural experiments, $PLC\delta4^{-/-}$ animals showed higher cold sensitivity in the acetone evaporation test, an effect that was inhibited by the TRPM8 antagonist PBMC ((*S*)-1-phenylethyl(2-aminoethyl)(4-(benzyloxy)-3 methoxybenzyl)carbamate). There was no difference between heat and mechanical sensitivity of $PLC\delta4^{-/-}$ and WT animals. Our data establish PLCδ4 as an important regulator of TRPM8 *in vivo*.

Methods

Xenopus oocyte isolation and electrophysiology

All animal procedures were approved by the Institutional Animal Care and Use Committee. *Xenopus laevis* oocytes were prepared using collagenase digestion, as described earlier (Lukacs *et al.* 2007). cRNA encoding TRPM8 and equal amounts of various PLC isoforms was injected using a nanolitre-injector system (Warner Instruments, Hamden, CT, USA). Oocytes were maintained in a solution containing (in mM) 87.5 NaCl, 5 KCl, 1 $MgCl_2$, 1.8 $CaCl_2$ and 5 Hepes for 2 days before experiments. For two-electrode voltage-clamp (TEVC) measurements, thin-wall inner filament-containing glass pipettes (World Precision Instruments, Sarasota, FL, USA) were filled with 3 M KCl in 1% agarose. To minimize Ca^{2+}-induced

Cl^- currents, measurements were conducted in a Cl^--free external solution containing 10 mM Hepes, 92 mM glutamate, 92 mM Na^+, 2 mM K^+ and 1 mM Mg gluconate (pH 7.4) as described earlier (Rohacs *et al.* 2005).

DRG neuron isolation and culture

Animal procedures were approved by the Institutional Animal Care and Use Committee. DRG neurons were isolated using the protocol of Malin *et al.* (2007) with slight modifications as described previously (Yudin *et al.* 2011; Lukacs *et al.* 2013). Briefly, DRG neurons were isolated from adult mice of either sex (2–4 months old) from offspring obtained after crossbreeding the TRPM8-GFP mouse line, expressing the green fluorescent protein (GFP) driven by the promoter of TRPM8 (Takashima *et al.* 2007) and PLCδ4$^{-/-}$ mice (Fukami *et al.* 2001), which resulted in a new line: PLCδ4$^{-/-}$-TRPM8-GFP. WT littermate PLCδ4$^{+/+}$-TRPM8-GFP mice were used in all control experiments. Animals were anaesthetized and perfused via the left ventricle with ice-cold Hank's buffered salt solution (HBSS; Invitrogen, Carlsbad, CA, USA) followed by decapitation. DRGs were collected from all spinal segments after laminectomy and maintained in ice-cold HBSS for the duration of the isolation. After isolation and trimming of dorsal and ventral roots, ganglia were incubated in an HBSS-based enzyme solution containing 2 mg ml^{-1} type I collagenase (Worthington, Lakewood, NJ, USA) and 5 mg ml^{-1} Dispase (Sigma, St Louis, MO, USA) at 37°C for 25–30 min, followed by repetitive trituration for dissociation. After centrifugation at 80 *g* for 10 min, cells were resuspended and plated on round coverslips pre-coated with poly-L-lysine (Invitrogen) and laminin (Sigma), allowed to adhere for 1 h and maintained in culture for 12–36 h before measurements in Dulbecco's modified Eagle's medium (DMEM:F12) supplemented with 10% FBS (Thermo Scientific, Waltham, MA, USA), 100 IU ml^{-1} penicillin and 100 μg ml^{-1} streptomycin and were kept in a humidity-controlled tissue culture incubator maintaining 5% CO_2 at 37°C.

Electrophysiology on DRG neurons

Whole cell voltage- or current-clamp recordings of menthol-, WS-12- and cold-evoked responses were performed on GFP-expressing DRG neurons using external solution with temperatures adjusted to 28–29°C. Patch clamp pipettes were pulled from borosilicate glass capillaries (Sutter Instruments, Novato, CA, USA) on a P-97 pipette puller (Sutter Instruments) and had a resistance of 2–5 MΩ. Neurons were continuously perfused with a normal bath solution containing (in mM): 137 NaCl, 5 KCl, 1 $MgCl_2$, 2 $CaCl_2$, 10 Hepes and 10 glucose, pH adjusted to 7.4 with NaOH. Intracellular solutions consisted of the following (in mM): 140 potassium gluconate, 1 $MgCl_2$, 5 Na_2ATP, 0.2 Na_2GTP, 0.2 EGTA, 10 Hepes, pH adjusted to 7.25 with KOH.

After formation of gigaohm resistance seals, the whole cell configuration was established and current or voltage signals were recorded with an Axopatch 200B amplifier (Axon Instruments, Union City, CA, USA). Cold stimulation was performed using a custom-made system with a temperature probe (Warner Instruments, Hamden, CT, USA) positioned in close proximity to the measured cell. All signals were sampled at 10 kHz and filtered at 5 kHz using the low-pass Bessel filter of the amplifier and digitized using pCLAMP 9.0 (Axon Instruments) and Digidata 1440 unit (Molecular Devices, Sunnyvale, CA, USA). In all experiments, cells that had a resting membrane potential more positive than −40 mV or a passive leak current more than 100 pA were discarded. Voltage-clamp recordings were performed at a holding potential of −60 mV and inward currents evoked by cold, menthol or WS-12 were recorded. Whole cell configuration was obtained in the voltage-clamp mode before proceeding to the current-clamp recording mode and series resistance was compensated > 70%. Because most DRG neurons are 'silent' (Wu & Pan, 2007) initial electrophysiological characteristics were determined in current-clamp mode with a graded series of 300 ms depolarizing and hyperpolarizing current pulses applied once per second ranging from −220 to 220 pA in 20 pA increments to elicit APs. The thresholds of APs were determined as the voltage at which the dV/dT function deviated from zero. Current-clamp recordings were then performed to study neuronal membrane excitability and AP firing properties during menthol stimulation.

Data were collected and analysed with pCLAMP, and further analysed and plotted with Origin 8.0 (Microcal Software Inc., Northampton, MA, USA). Most reagents were purchased from Sigma, unless otherwise indicated, stock of (–)-menthol and capsaicin were made in ethanol. WS-12 was purchased from Bio-techne/Tocris (Ellisville, MO, USA). All dilutions were prepared on the day of the experiment.

Western blot

Western blot experiments were performed to measure TRPM8 protein expression levels in DRG-s from WT and PLCδ4$^{-/-}$ animals. Ganglia were removed as described and the collected tissue was lysed using the freeze–thawing method and homogenized in 150 μl of buffer (pH 7.5) containing 50 mM Tris, 150 mM NaCl, 1 mM EDTA, 1% TritonX-100, 1 mM phenylmethylsulfonyl fluoride (Sigma), 2 mM Na_3VO_4, 0.2% SDS, 5% 2-mercapthoethanol, supplemented with 1% of protease inhibitor cocktail ProteCease-100 (BD Biosciences, Franklin Lakes, NJ, USA) and 1% Complete mini

(Roche, Indianapolis, IN, USA). At the final step the lysates were centrifuged at 14,400 *g* for 40 min at 4°C and supernatants were used for experiments. Total protein concentrations were measured with a Bradford protein assay (Sigma); a standard curve was obtained using known BSA concentrations; protein concentrations were extrapolated from the standard curve. Then 25 μg of protein was resolved on a 4–20% SDS-PAGE gradient gel (Bio-Rad, Hercules, CA, USA). Proteins were transferred to polyvinylidene fluoride membrane (Trans-Blot Turbo, Bio-Rad), using a semi-dry transfer apparatus (Bio-Rad) and blocked in 5% skimmed milk, 0.05% Tween 20 in TBS, and incubated overnight at 4°C with 1:1000 anti-TRPM8, rabbit monoclonal antibody (Origene, Rockville, MD, USA; cat. no. TA307827) and 1:1000 anti-GAPDH, rabbit monoclonal antibody (Cell Signaling, Danvers, MA, USA; cat. no. 2118). The blots were then incubated with an HRP-conjugated anti-rabbit secondary antibody (1:2000, Jackson ImmunoResearch, West Grove, PA, USA) for 60 min at room temperature, and developed in ECL (enhanced chemiluminescence) solution (Thermo Scientific). The standardization ratio of TRPM8 to GAPDH band density was used to calculate the change in TRPM8 expression. Western blots images were analysed by densitometry in ImageJ (http://rsb.info.nih.gov/ij/index.html).

Evaporative cooling assay (acetone test)

All animals were housed three per cage maximum, on a 12 h light/dark cycle with food and water available *ad libitum;* average animal weight in the PLCδ4$^{-/-}$ group was 28.3 $\pm$ 0.8 g (n = 11) and in the WT group it was 29.0 $\pm$ 0.9 g (n = 12). One day before experiments animals were transferred to the experimental room for acclimatization, separated in individual cages and provided food and water *ad libitum*. The evaporative cooling assay was performed according to Knowlton *et al.* (2011) with some modification as follows: in the cooling assay we used only male animals, and experiments were at 11:00–16:00 h at room temperatures (26–27°C). Before experiments, mice were acclimated for 40 min in a plastic chamber with a mesh floor. A microsyringe with a piece of rubber tubing attached to the needle was filled with 50 μl acetone and all volume applied to the mouse's hind paw. Mice were tested six times for 5 min with an inter-stimulation period of 5 min, every time alternating paws between acetone applications. The six trials on individual animals were averaged and taken as one data point for the statistical evaluation. The first 10 s of activity was disregarded as a response to the initial acetone application. Responses were recorded by an observer blind to the genetic background. The following behavioural responses were measured: number and duration of licking of the treated paw and duration of limping (dragging paw). For *in vivo* intraperitoneal injections, the initial stock of 30 mg ml^{-1} PBMC (Focus Biomolecules, Plymouth Meeting, PA, USA) in DMSO solution, or equal volume of DMSO as a control were diluted 30$\times$ in a sterile vehicle solution of 10% PEG-200 (Sigma-Aldrich), 2% Tween-80 (Amresco, Cleveland, OH, USA) in 0.9% NaCl. The final dose of the injected PBMC was 10 mg kg^{-1}. The animals were allowed to settle for 1 h following PBMC or vehicle injections. Every animal was subject initially to vehicle injection for control experiments, followed 7–10 days later by PBMC injection.

Mechanical (von Frey) test

Behavioural experiments to test for mechanical sensitivity were performed as described earlier (Zhao *et al.* 2013). Briefly, mice were acclimated to the testing environment 1 day prior to testing; we used male mice for these experiments. On the testing day, mice were individually placed in a chamber that provided enough room for the mouse to turn around, but not to stand on its hind legs. The chambers were placed on an elevated wire mesh platform. The mice were left to acclimate for 1 h prior to testing. Two von Frey filaments (0.07 and 0.4 g) were applied to each hind paw a total of ten times and the number of positive responses (a quick withdrawal of the paw, biting and/or licking of the paw) were recorded. The number of positive responses out of ten stimulations is expressed as a percentage (paw withdrawal frequency). Responses in the left and right paws were not different, so the data on the two paws were pooled, and the average data are plotted in the figure.

Hargreaves test

Behavioural experiments to test for heat sensitivity were performed as described earlier (Zhao *et al.* 2013); we used male mice for these experiments. Mice were placed in the same chambers as for the von Frey test on a glass platform connected to a Model 336 Analgesia Meter (IITC Inc. Life Science Instruments, Woodland Hill, CA, USA) and were left to acclimate for 1 h. The intensity was set such that the temperature of the light source started at 38°C and reached 52°C after 8 s of administration. Each paw was exposed to the light source for five trials, each trial separated by 10 min. The time between the beginning of the light administration and a positive response (quick withdrawal of paw, biting and/or licking of the paw) was recorded and represents the paw withdrawal latency (seconds). Responses in the left and right paws were not different, so the data on the two paws were pooled, and the withdrawal latencies for each mouse were averaged before statistical summary, and represented as one data point.

Tail flick test

The same mice, which were used for the Hargreaves test, were rested overnight and then subjected to a tail-immersion test (water bath modification). Two centimetres of the tail was dipped into a water bath maintained at 48.0°C, and a vigorous tail flick was considered a positive response, and the latency of response in seconds was recorded and plotted. In each mice two experiments were performed 5 min apart, and the withdrawal times were averaged before statistical summary.

Statistics

Data are presented as mean ± SEM. All comparisons between means were tested for significance using Student's paired *t*-test or ANOVA. $P < 0.05$ was considered to be statistically significant.

Results

PLCδ4 accelerates Ca^{2+}-dependent desensitization of TRPM8 in a heterologous expression system

We showed earlier that coexpression of PLCδ1 with TRPM8 in *Xenopus* oocytes markedly accelerated desensitization of the channel (Rohacs *et al.* 2005). The highest expressing highly Ca^{2+}-sensitive PLC isoform in DRGs, however, is PLCδ4 (Lukacs *et al.* 2013). First we tested if this isoform can also accelerate TRPM8 desensitization. Figure 1 shows that any of the three PLCδ isoforms, PLCδ1, PLCδ3 or PLCδ4, markedly accelerated Ca^{2+}-dependent desensitization of TRPM8

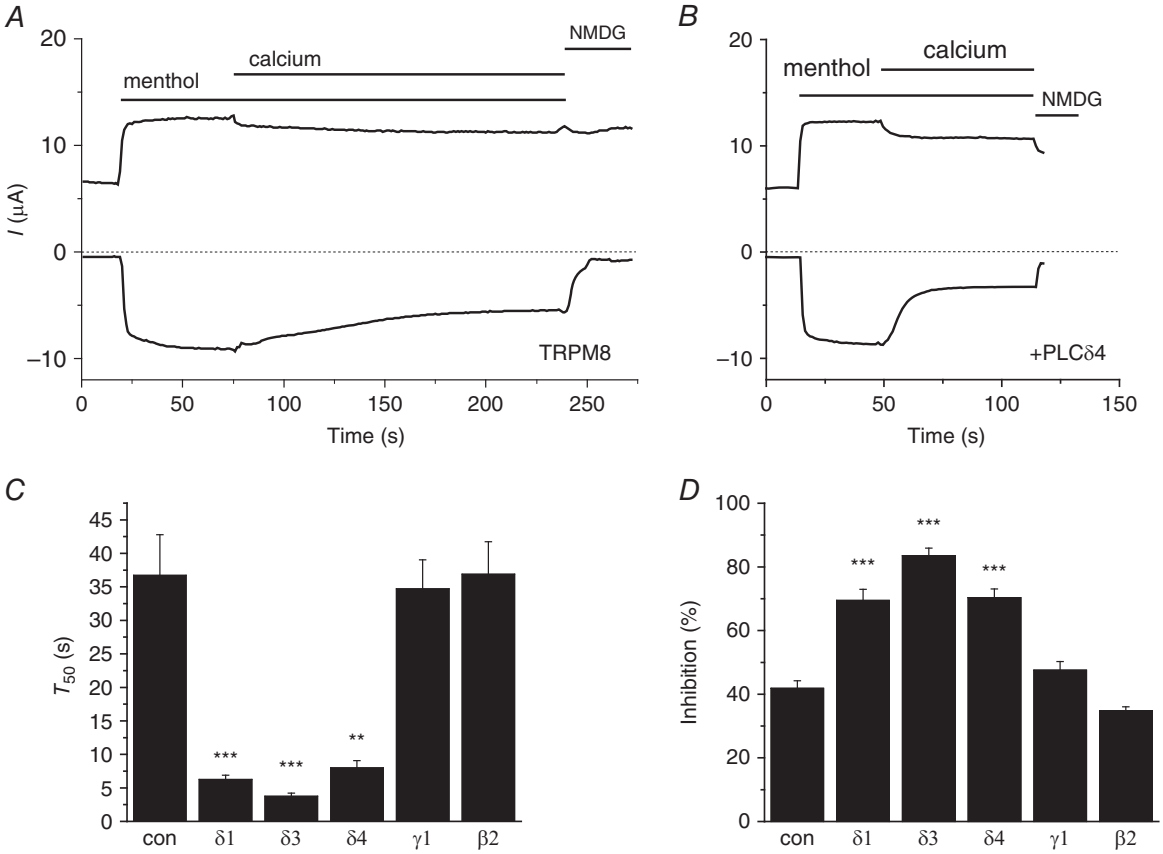

Figure 1. PLCδ isoforms accelerate Ca^{2+}-induced desensitization of TRPM8 in *Xenopus* oocytes
Two electrode voltage-clamp experiments were performed as described in the Methods using a ramp protocol from −100 to 100 mV repeated every second. *A*, representative trace from an oocyte expressing TRPM8; currents at −100 and 100 mV are plotted, and zero current is indicated by the dotted line. The applications of 500 μM menthol and 2 mM Ca^{2+} are shown by the horizontal lines. At the end of the experiment the solution was replaced by an *N*-methyl-D-glucamine (NMDG)-based solution to inhibit TRPM8 currents. *B*, similar representative measurement in an oocyte co-expressing TRPM8 and PLCδ4. *C*, summary of the T_{50} of Ca^{2+}-induced inhibition at −100 mV in oocytes coexpressing TRPM8 and various PLC isoforms. *D*, summary of the level of inhibition upon Ca^{2+} application at −100 mV in oocytes coexpressing TRPM8 and various PLC isoforms ($n = 4$–7).

during menthol application. Representative members of the other two classical PLC groups, PLCβ2 and PLCγ1, on the other hand, had no effect.

Small, but not medium–large, PLCδ4$^{-/-}$ DRG neurons are more sensitive to cold and menthol in whole cell voltage-clamp experiments

To investigate the possible role of PLCδ4 in modulating the activity of native TRPM8 channels, we performed experiments on DRG neurons isolated from PLCδ4$^{-/-}$ mice (Fukami *et al.* 2001) and WT littermates. Both PLCδ4$^{-/-}$ and WT animals also expressed GFP, driven by the promoter of TRPM8, allowing visual identification of TRPM8-positive neurons by green fluorescence; GFP-positive neurons amounted to 5–7% of the total (Takashima *et al.* 2007).

In whole cell voltage-clamp experiments at −60 mV holding potentials, two subsequent applications of 500 μM menthol (60 s duration each) induced inward currents in the majority of GFP-positive neurons. Consistent with earlier results, current amplitudes decreased during agonist stimulation (desensitization) (Fig. 2). In both the PLCδ4$^{-/-}$ and the WT groups we identified two TRPM8-positive neuronal subpopulations based on their cell body size and responses to agonists. In small WT neurons (<15 pF, $n = 24$) (Fig. 2*A*, *B*) current densities for both menthol applications were significantly higher compared to the medium–large neurons (>15 pF, $n = 19$) (Fig. 2*C*, *D*), $P = 0.0004$ for the first menthol pulse. This

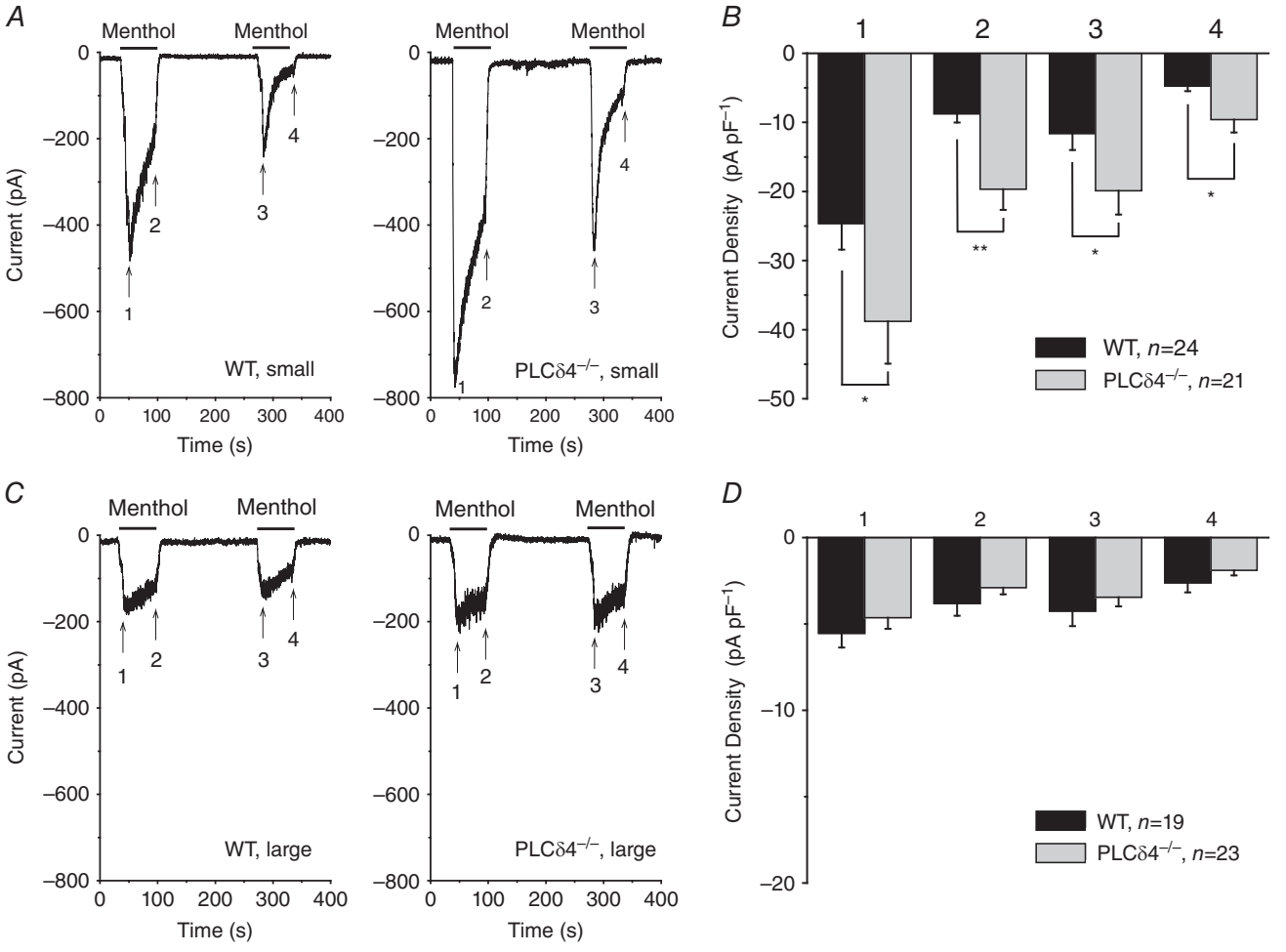

Figure 2. Menthol-induced inward currents in whole cell voltage-clamp experiments in GFP-positive WT and PLCδ4$^{-/-}$ DRG neurons
Experiments were performed as described in the Methods (V_h −60 mV). *A*, representative responses of a small WT (10 pF, left) and a PLCδ4$^{-/-}$ DRG neuron (9 pF, right) to 500 μM menthol (60 s pulse duration). *B*, summary of current densities from small DRG neurons (4–15 pF) in whole cell voltage-clamp, at the time points indicated in *A* by the arrows. *C*, representative responses of a large WT DRG neuron (17 pF, left) and PLCδ4$^{-/-}$ neuron (21 pF, right) to the application of 500 μM menthol. *D*, summary of current densities from large WT and PLCδ4$^{-/-}$ DRG neurons (>15 pF). *P<0.05; **P<0.01.

difference in menthol-induced currents was also observed between small ($n = 21$) and larger PLC$\delta4^{-/-}$ neurons ($n = 23$), $P = 7.5 \times 10^{-7}$ for the first menthol pulse.

Analysis of the neuronal responses based on genetic background revealed that in small PLC$\delta4^{-/-}$ neurons menthol-induced currents were significantly larger compared to the same size WT neurons (Fig. 2*A*, *B*). In neurons with larger cell bodies the differences in the current amplitudes between two genetic strains were negligible (Fig. 2*C*, *D*). Desensitization of the menthol-induced currents was observed in both PLC$\delta4^{-/-}$ and in WT neurons. Acute desensitization, on average, was less in small PLC$\delta4^{-/-}$ neurons than in WT. By the end of the first menthol application the currents decreased to 56 ± 4% of the peak value in small PLC$\delta4^{-/-}$ neurons, compared to 46 ± 4% in small WT neurons, but this difference did not reach the 0.05 cutoff for statistical significance ($P = 0.06$). To identify the presence of transient receptor potential vanilloid 1 (TRPV1) channels in these neurons, we applied a short pulse of capsaicin (500 nM) at the end of each experiment. The majority of the small neurons (53 from 59) responded to capsaicin (500 μM), while only 3 out of 33 larger neurons responded to the TRPV1 agonist. Figure 3 demonstrates dependence of the menthol-induced current densities on cell size (capacitance in pF) and capsaicin sensitivity in these two groups.

To use cold as a stimulus, the external solution with temperatures of 28–29°C was quickly exchanged for a solution with a temperature of about 10°C (drop to minimum temperature in 3–4 s). Similar to menthol-induced TRPM8 activation, cold-induced current densities in small neurons from PLC$\delta4^{-/-}$ animals ($n = 29$) were larger compared to WT neurons ($n = 28$), but only in the initial phase of the inward currents. Figure 4*A* and *B* shows two representative traces obtained from a WT and a PLC$\delta4^{-/-}$ neuron, and Fig. 4*C* shows statistical analysis for this set of experiments. To confirm that the effect of PLC$\delta4$ deletion was not due to the increased number of functional TRPM8 channels, we applied a supramaximal stimulus at the end of each experiment, using 2 mM menthol, the highest concentration that can be dissolved in an aqueous buffer, cooled to a temperature similar to the cold stimulus we used for TRPM8 activation. Currents induced by this supramaximal stimulation were not different between the two genetic groups, implying that the number of functional channels was similar between the WT and PLC$\delta4^{-/-}$ neurons. Similarly, the temperature thresholds of TRPM8 channel activation were almost identical between PLC$\delta4^{-/-}$ and WT small neurons, 26.7 ± 0.4 and 26.0 ± 0.7°C, respectively.

To confirm the similar TRPM8 protein levels in WT and PLC$\delta4^{-/-}$ DRG neurons, we also performed Western blot from the DRG lysates using an anti-TRPM8 antibody. Our data show similar TRPM8 levels for both WT and PLC$\delta4^{-/-}$ groups (Fig. 5).

Comparison of small and larger TRPM8-positive neurons in current clamp experiments

Our data so far show significant differences in agonist-induced TRPM8 current amplitudes in voltage-clamp experiments between the PLC$\delta4^{-/-}$ and WT genetic groups, as well as between small and larger neurons. Next we tested the difference in neuronal excitability and AP properties in these groups of DRG

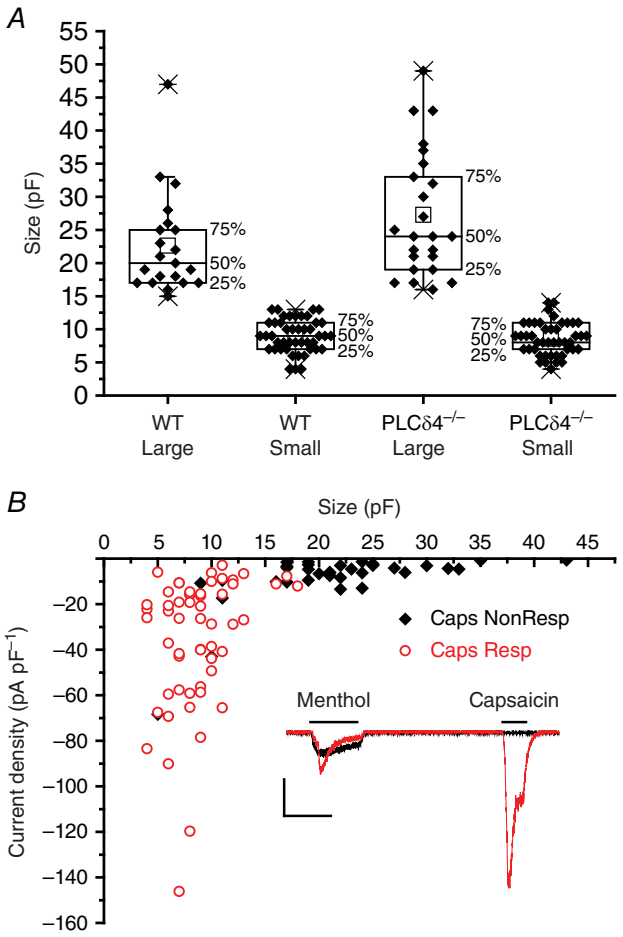

Figure 3. Neuronal size distribution and capsaicin sensitivity in TRPM8-positive DRG neurons
A, cell body size distribution in two neuronal populations: small (4–15 pF) and larger neurons (>15 pF) obtained in whole cell voltage-clamp experiments using 500 μM menthol as a stimulus. Whole cell capacitance values (mean [small box], and percentiles) are plotted to represent individual neuron sizes. *B*, dependence of menthol-induced current density on cell size (capacitance). Capsaicin-sensitive neurons are marked by red circles and non-responding cells by black diamonds. Inset shows superimposed responses of two cells, one small neuron responding to 500 nM capsaicin, and one larger one not responding to capsaicin; scale bars: 200 pA and 60 s.

neurons in current-clamp measurements. In every TRPM8-expressing neuron first we recorded AP firing properties in response to depolarizing current injections up to +220 pA and hyperpolarizing pulses up to −220 pA. Figure 6*A* and *B* shows two representative current-clamp recordings from small WT and PLC$\delta4^{-/-}$ DRG neurons, with current injections ranging from −220 to +220 pA. For the positive current injection step we included only +20 and +220 pA pulses (marked in red) due the high level of activity at positive voltages. For the small neurons in both WT ($n = 33$) and PLC$\delta4^{-/-}$ ($n = 22$), initial depolarization (20–60 pA) induced a similar fast increase in frequency of firing of APs. Higher levels of depolarizing current injections, after reaching the peak, lead to the reduction in AP frequency for the WT neurons, while PLC$\delta4^{-/-}$ neurons kept a high level of firing in all ranges of injected currents (Fig. 6*E*). Hyperpolarizing pulses for both WT and PLC$\delta4^{-/-}$ neurons showed very similar responses both at the peak and at steady state (Fig. 6*C*, *D*). They also revealed almost identical voltage- and time-dependent rectification (sag) characteristic identified to be specific for the cold-sensitive neurons (Viana *et al.* 2002), and the rebound firing at the end of a hyperpolarizing pulse that was demonstrated to depend on the presence of I_h (Orio *et al.* 2009).

Depolarizing current injections in medium–large neurons for both WT ($n = 10$) and PLC$\delta4^{-/-}$ ($n = 9$) induced APs with variable frequencies, but generally excitability in larger neurons was significantly smaller (Fig. 7*E*), requiring higher levels of current injection for

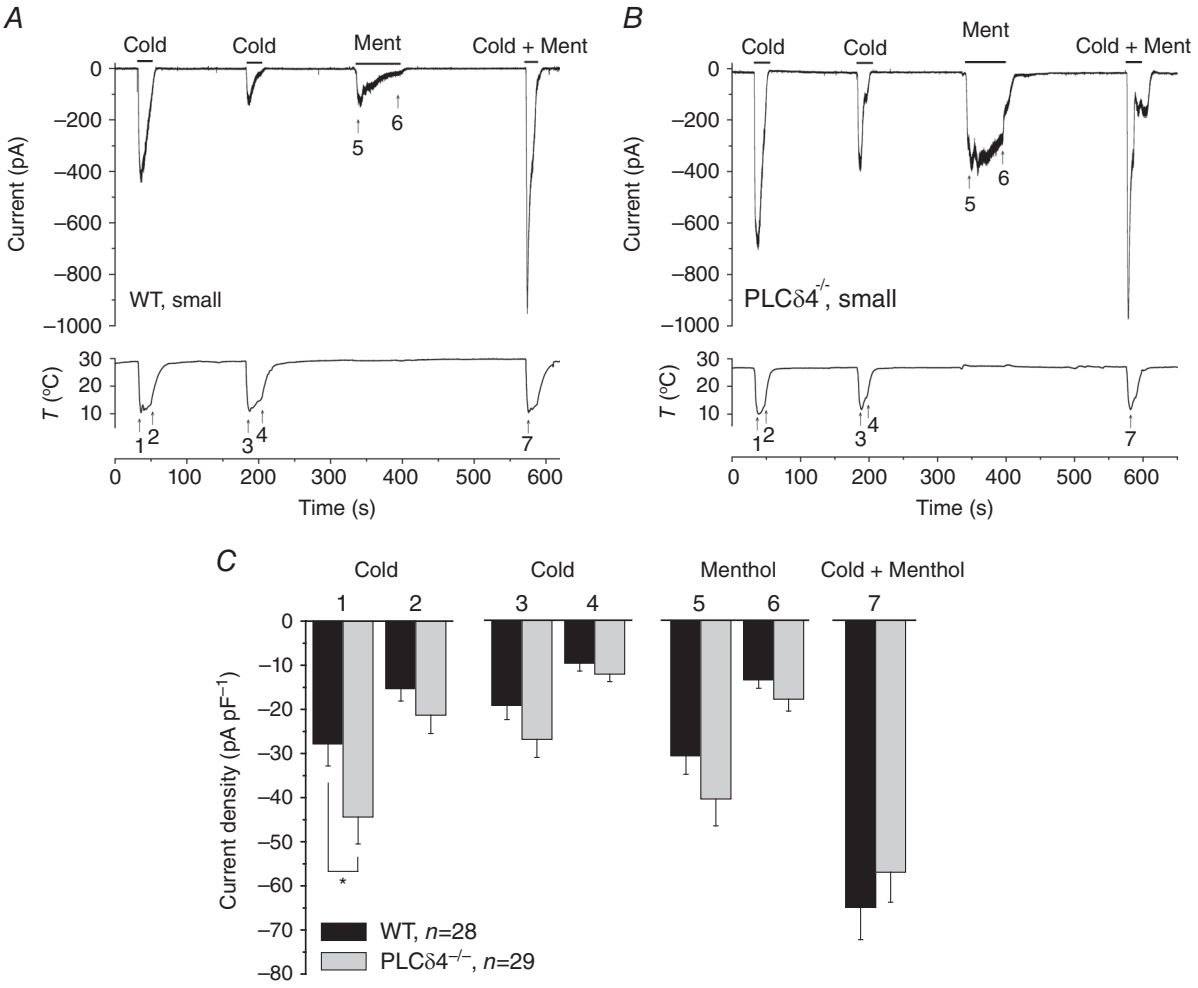

Figure 4. Cold-induced inward currents in whole cell voltage-clamp recordings in small GFP-positive WT and PLC$\delta4^{-/-}$ DRG neurons
Experiments were performed as described in the Methods. *A* and *B*, representative responses at V_h −60 mV during two subsequent cold pulses in a WT (6 pF) and a PLC$\delta4^{-/-}$ (7 pF) DRG neuron. Lower traces show bath temperature measured with a temperature probe placed in close vicinity of the cell. Neurons were also stimulated with menthol (500 μM) and as a saturating agonist we used 2 mM menthol chilled to similar temperature as the cold stimulus (Cold + menthol). *C*, summary of current densities in the subpopulation of small DRG neurons (4–15 pF), at the time points indicated by the arrows in *A* and *B*. *P<0.05.

generating APs than in small neurons. In the representative responses in Fig. 7*A* and *B* we included only +100 and +220 pA current injection steps (marked in red) with corresponding cell responses. Responses to hyperpolarizing current pulses for both WT and PLCδ4$^{-/-}$ large neurons were also very similar both at the peak of response and at steady state (Fig. 7*C*, *D*), but demonstrated less sag level compared to the small neurons and complete absence of rebound activation. The similar voltage responses to hyperpolarizing current for WT and PLCδ4$^{-/-}$ neurons could imply that deletion of PLCδ4 does not influence I_h ionic conductances. Analysis of APs revealed very similar properties for PLCδ4$^{-/-}$ and WT small neurons that were different from the properties of the large neurons; Fig. 7*F* demonstrates superimposed APs typical for small neurons and large ones. Small neurons had narrow APs while large neurons had broader APs and displayed a hump at its repolarization phase (15 from 19 large neurons demonstrated this AP shape). Other membrane parameters including AP duration, amplitude, threshold and after-hyperpolarization (AHP) duration and its peak values were found to be not significantly different between WT and PLCδ4$^{-/-}$ neurons (Table 1). Input resistance and inward rectification index (Viana *et al.* 2002) were also not different between WT and PLCδ4$^{-/-}$ neurons (Table 1). AP duration, AHP amplitude and duration, input resistance and inward rectification index showed significant differences between small and medium–large neurons, both in the WT and the PLCδ4$^{-/-}$ groups (Table 1).

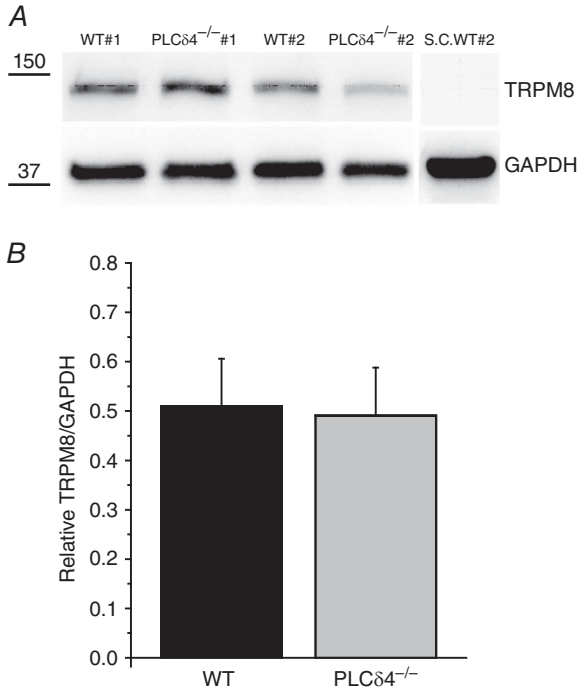

Figure 5. TRPM8 protein levels are similar in WT and PLCδ4$^{-/-}$ DRG neurons
Western blots demonstrating TRPM8 (~140 kDa) expression level (upper panel) obtained from two pairs of WT and PLCδ4$^{-/-}$ DRG neurons and GAPDH (~40 kDa) protein expression that was used as a loading control. As a negative control we used a protein sample obtained from the spinal cord (S.C.) simultaneously with DRG from one of the experimental animals. The lower panel shows the relative level of TRPM8 expression compared to GAPDH in WT and PLCδ4$^{-/-}$ animals. Protein blots were measured by densitometry, $n = 6$ for each genetic group.

Small PLCδ4$^{-/-}$ DRG neurons are more sensitive than WT to menthol in current clamp experiments

After measurements of the AP parameters, we recorded responses to menthol (500 μM) in the current-clamp mode. We observed that both PLCδ4$^{-/-}$ ($n = 26$) and WT ($n = 37$) small neurons had more positive resting membrane potentials compared to the large ones (Fig. 8; $P = 5.11 \times 10^{-9}$ for WT and $P = 0.016$ for PLCδ4$^{-/-}$). In small PLCδ4$^{-/-}$ neurons, menthol applications induced significantly larger depolarizations and generation of APs with frequencies significantly higher compared to WT small neurons (Fig. 8*A*–*D*). It is noteworthy that AP firing was observed at the beginning of agonist application, during the initial phase of membrane potential increase (Fig. 8*A*, *C*). Further firing of neurons was completely abolished while depolarization reached its maximum values.

Consistent with our voltage-clamp data, for the large neurons we did not find any difference in the responses to menthol between PLCδ4$^{-/-}$ ($n = 9$) and WT ($n = 14$) neurons in current clamp measurements (Fig. 8*E*–*H*). Depolarization levels during the first menthol application were very similar and for the second one it was almost identical between large WT and PLCδ4$^{-/-}$ neurons (Fig. 8*F*). Although AP number for large PLCδ4$^{-/-}$ neurons was higher than for WT neurons (Fig. 8*H*), the effect was not significant and for both WT and PLCδ4$^{-/-}$ large neurons this parameter was dramatically lower compared to the small neurons (Fig. 8*D*).

Small PLCδ4$^{-/-}$ DRG neurons show increased current responses to the specific TRPM8 agonist WS-12

Menthol, while often used as a TRPM8 agonist, may also activate other ion channels, including transient receptor potential ankyrin 1 (TRPA1) (Karashima *et al.* 2007; Liu *et al.* 2013). Therefore we performed experiments with a submaximal concentration of WS-12, a more specific TRPM8 agonist (Bodding *et al.* 2007; Liu *et al.* 2013), which does not activate TRPA1 (Sherkheli *et al.* 2008). Figure 9 shows that small GFP-positive DRG neurons responded with an inward current to the application of 1 μM WS-12, and responses of PLCδ4$^{-/-}$ neurons were significantly larger than those in WT neurons. Similarly,

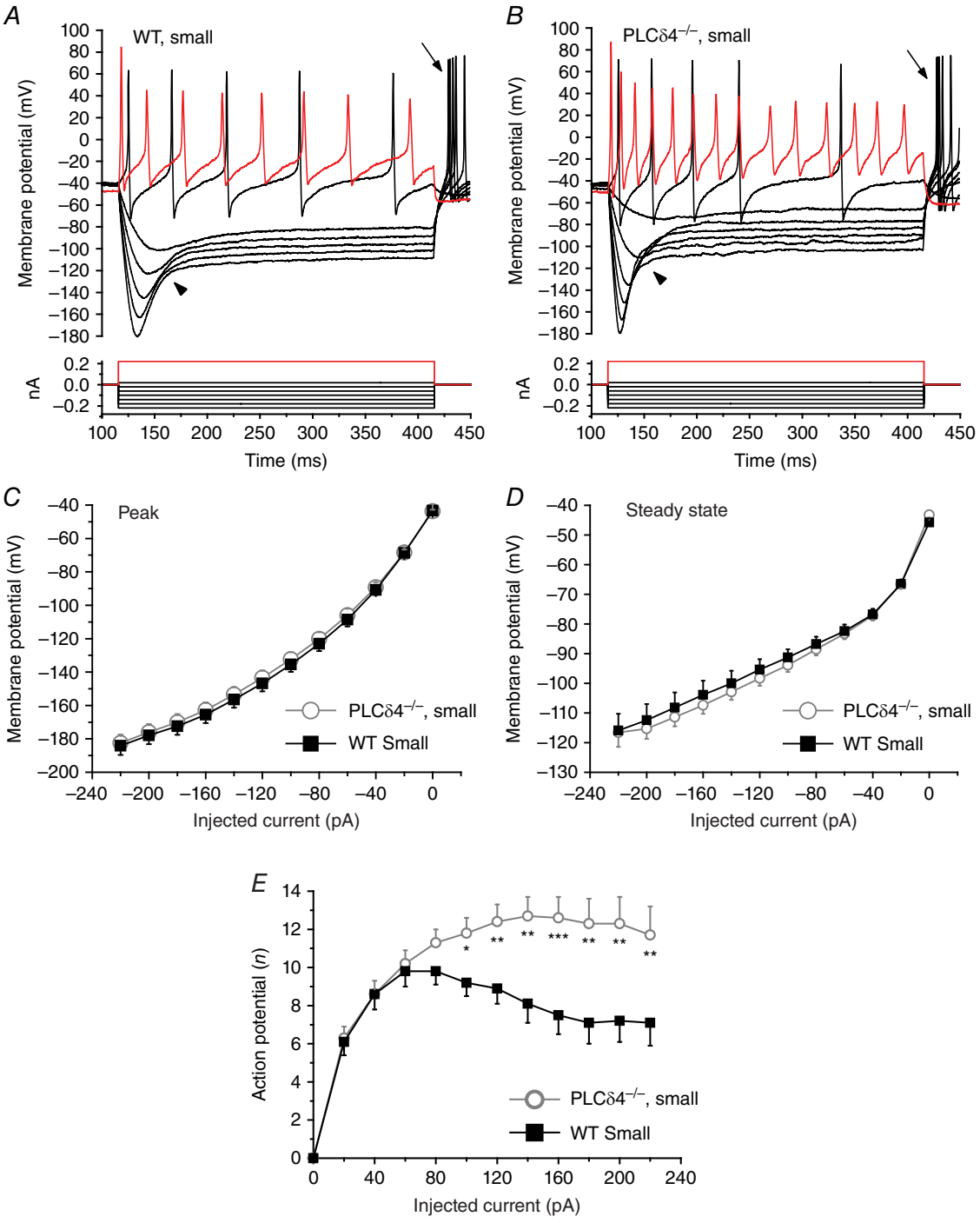

Figure 6. Current-clamp recordings from small GFP-positive DRG neurons stimulated with current injections

Experiments were performed as described in the Methods. *A* and *B*, representative recordings from WT and PLC$\delta4^{-/-}$ neurons. From resting membrane potentials, 300 ms current injection steps were applied ranging from −220 to +220 pA with a 20 pA step once every second. Responses were characterized by strong voltage- and time-dependent rectification (sag) during hyperpolarization steps (arrowhead); note presence of rebound spikes after hyperpolarization pulse (arrow) and fast AP firing during positive currents injections. Bottom part shows the stimulus protocol: positive steps +20 and +220 pA (marked in red) and negative current steps injection up to −220 pA. *C* and *D*, summary of negative current injections at the peak (*C*) and at the end of the hyperpolarizing stimulus (steady state) (*D*). *E*, summary of trains of AP in response to positive current injections in small DRG neurons ($n = 26$ for WT and $n = 22$ for PLC$\delta4^{-/-}$). *$P<0.05$; **$P<0.01$, ***$P<0.001$.

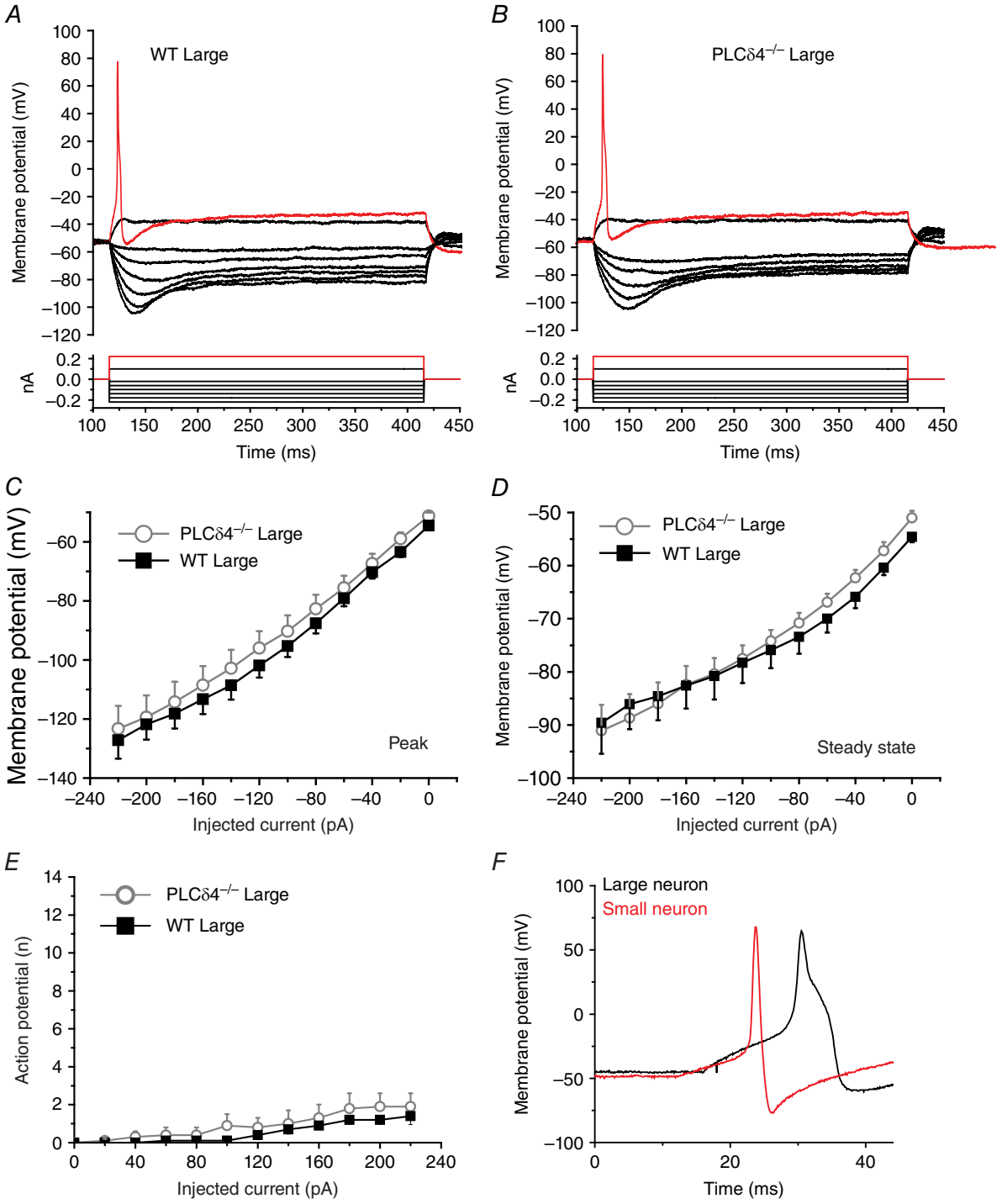

Figure 7. Current-clamp recording from larger GFP-positive DRG neurons stimulated with current injections

Experiments were performed as described in the Methods identical to that described in Fig. 6 for small neurons. *A* and *B*, representative recording from large WT and PLC$\delta4^{-/-}$ neurons. From the resting membrane potentials, 300 ms current injection steps were applied ranging from −220 to +220 pA with 20 pA increments. Rectification was less profound compared to small neurons, and rebound spikes were absent after hyperpolarization pulses. Bottom part shows the stimulus protocol. *C* and *D*, summary of negative current injections at the peak (*C*) and at the end of the hyperpolarizing stimulus (steady state) (*D*). *E*, summary of APs at different current injection levels induced mostly at the maximum level of positive current injection pulses for both WT (n = 10) and PLC$\delta4^{-/-}$ neurons (n = 9). *F*, representative individual APs on a shorter time scale for a large and a small neuron.

Table 1. Electrophysiological properties of TRPM8 WT and PLCδ4$^{-/-}$ (KO) neurons

Type of neurons	AP amplitude (mV)	AP threshold (mV)	AP duration (ms)	AHP amplitude (mV)	AHP duration (ms)	Input resistance (MΩ)	Inward rectification index
Small WT, $n = 33$	86.5 ± 2.11 NS *vs.* WT Large	−20.2 ± 0.51 NS *vs.* WT Large	1.1 ± 0.04 NS *vs.* WT Large	−47.8 ± 1.37 $P = 0.0033$ *vs.* WT Large	4.1 ± 0.31 $P = 4.7 \times 10^{-11}$ *vs.* WT Large	325.4 ± 26.7 $P = 0.015$ *vs.* WT Large	62.2 ± 0.8 $P = 0.0001$ *vs.* WT Large
Small KO, $n = 23$	89.4 ± 2.47 NS *vs.* KO Large	−20.8 ± 0.63 NS *vs.* KO Large	1.1 ± 0.07 $P = 0.013$ *vs.* KO Large	−48.8 ± 1.94 $P = 0.016$ *vs.* KO Large	3.8 ± 0.26 $P = 5.6 \times 10^{-9}$ *vs.* KO Large	306.3 ± 29.1 $P = 0.048$ *vs.* KO Large	60.0 ± 1.3 $P = 0.006$ *vs.* KO Large
Large WT, $n = 11$	93.7 ± 3.88	−21.0 ± 1.21	1.3 ± 0.09	−39.3 ± 1.4	12.6 ± 1.67	200.4 ± 14.4	49.5 ± 1.6
Large KO, $n = 9$	85.2 ± 4.18	−19.1 ± 1.21	1.5 ± 0.19	−40.1 ± 2.31	12.6 ± 1.66	209.1 ± 9.2	52.5 ± 2.4

AP, action potential; AP duration, action potential width measured at 50% amplitude; AP threshold, the minimal depolarization voltage to produce an AP; AHP duration, width measured at 50% amplitude. There were no significant differences between WT and PLCδ4$^{-/-}$ neurons in any of the parameters. Differences between small and large neurons are noted.

the responses of PLCδ4$^{-/-}$ neurons to 10 μM menthol were significantly larger than those observed in WT neurons (Fig. 9). Consistent with our earlier results shown in Fig. 2, responses to 500 μM menthol were also larger in these PLCδ4$^{-/-}$ neurons than in WT cells (Fig. 9). With the exception of one cell (1 out of 28 tested), small GFP-positive neurons did not respond to the TRPA1 agonist mustard oil (50 μM) (Fig. 9).

Our electrophysiology data show that the vast majority of GFP-positive cells do not respond to mustard oil. We also performed Ca^{2+} imaging experiments to further characterize menthol responses of our DRG preparation (data not shown). Consistent with our electrophysiology data, the vast majority of GFP-positive cells (117/124) did not respond to mustard oil (50 μM). From the GFP-negative population, 85% of the mustard oil responsive cells (172/202 cells) also responded to menthol (500 μM) but only two cells to WS-12 (1 μM). The amplitudes of these menthol responses were much smaller than those in GFP-positive cells. None of the mustard oil non-responsive GFP-negative cells responded to menthol or WS-12 (>400 cells tested). These data together indicate that non-TRPM8-mediated effects of menthol are restricted to mustard oil-responsive (TRPA1-positive) cells, which, consistent with earlier reports (Story *et al.* 2003), have negligible overlap with TRPM8-expressing (GFP-positive) neurons.

PLCδ4$^{-/-}$ mice are more sensitive to evaporative cooling

Our electrophysiological experiments demonstrate differences in response to cold and TRPM8 agonists between small WT and PLCδ4$^{-/-}$ sensory neurons. Enhanced TRPM8 channel activity in PLCδ4$^{-/-}$ neurons at the cellular level could lead to different behavioural responses *in vivo*. TRPM8$^{-/-}$ mice show reduced behavioural responses to evaporative cooling induced by acetone (Dhaka *et al.* 2007). Therefore, we performed this behavioural test and measured the duration and number of nocifensive events (licking, biting and guarding) of the treated paw. Also in preliminary trials we noticed changes from normal posture to limping on, or dragging, the treated paw in the first minute after acetone application. We found higher cold sensitivity for both measured parameters in PLCδ4$^{-/-}$ mice compared to WT (Fig. 10). For licking of the treated paw both the duration and the number of lickings were significantly higher compared to WT mice (18.1 ± 1.3 s *vs.* 10.6 ± 0.8 s, $P = 0.00005$ and 7.6 ± 0.5 *vs.* 5.6 ± 0.4, $P = 0.0024$) (Fig. 10*A*, *C*). For limping on the treated paw this difference was smaller, but still significant, duration changing from 17.5 ± 1.7 s in PLCδ4$^{-/-}$ to 13.6 ± 0.8 s in WT ($P = 0.037$; Fig. 10*D*).

Next we set out to test whether the difference between PLCδ4$^{-/-}$ and WT animals was due to TRPM8 activity. The genes for TRPM8 and PLCδ4 are very close to each other on chromosome 1 in mice, making the generation of double knockout mice essentially impossible. Thus, we tested the effect of the pharmacological blockade of TRPM8 channels by the TRPM8 antagonist PBMC, which was shown earlier to attenuate the responses to acetone in this assay (Knowlton *et al.* 2011). We gave intraperitoneal injections of 10 mg kg^{-1} PBMC and measured behavioural responses 1 h after injection using the same animals that we used in control (I.P. injection of vehicle) 1 week earlier. Pretreatment with PBMC reduced cold-induced responses in both groups, but the inhibition was larger in PLCδ4$^{-/-}$ animals. In the PLCδ4$^{-/-}$ group licking of the treated paws after PBMC decreased from

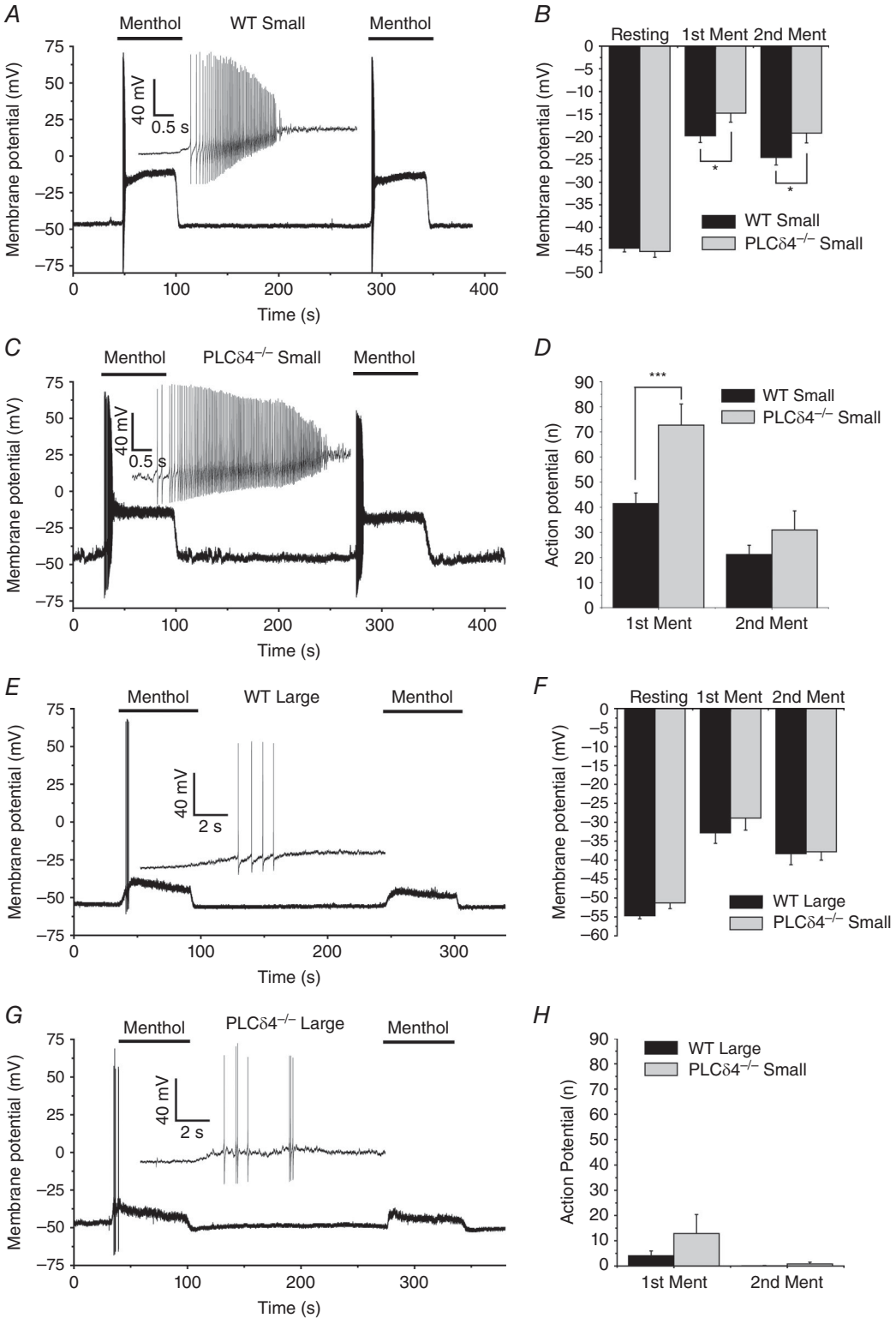

Figure 8. Menthol-induced neuronal activation in current-clamp experiments in GFP-positive WT and PLCδ4$^{-/-}$ DRG neurons

A and *C*, representative current-clamp recording from small DRG neurons that responded with high level of AP generation to 500 μM menthol (60 s application). Inset shows an expanded time scale for the initial phase of menthol-induced activation. *B*, analysis of the menthol-induced changes in membrane potential before and during activation in small WT and PLCδ4$^{-/-}$ neurons. *D*, summary of the number of APs for the small WT and PLCδ4$^{-/-}$

18.1 ± 1.3 to 11.1 ± 1.1 s. (38% inhibition, $P = 0.0005$) and in the WT group this parameter changed from 10.6 ± 0.8 to 7.56 ± 0.7 s (28% inhibition, $P = 0.001$) (Fig. 10*A*). Two-way ANOVA showed a significant interaction between TRPM8 antagonist and genotype ($P = 0.042$). For the parameter of limping in the PLC$\delta4^{-/-}$ group the initial value decreased from 17.5 ± 1.7 to 11.9 ± 0.9 s. (32% inhibition, $P = 0.0082$) and in WT it changed from 13.6 ± 0.8 to 12.1 ± 0.6 s (11% inhibition, NS) (Fig. 10*D*). For the limping parameter, there was a significant interaction between genotype and TRPM8 inhibitor with two-way ANOVA ($P = 0.027$).

For PBMC it was demonstrated that this reagent at this dose did not produce a change in core temperature beyond that observed with circadian rhythms (35.3–38.0°C) and only a higher concentration of PBMC (20 mg kg^{-1}) led to a significant drop in core body temperature and affected behaviour by hypothermia (Knowlton *et al.* 2011). Therefore, this reduction in observed cold-induced animal responses could be explained by inhibition of TRPM8 activity and the higher level of inhibition in PLC$\delta4^{-/-}$ animals corresponds well with higher level of neuronal activity that we observed in voltage and current clamp experiments.

neurons. *E* and *G*, representative responses recorded from larger WT and PLC$\delta4^{-/-}$ DRG neurons to menthol application. Inset shows an expanded time scale for the initial phase of menthol-induced activation. *F*, analysis of the menthol-induced changes in membrane potential before and during activation in large WT and PLC$\delta4^{-/-}$ neurons. *H*, summary of the number of menthol-induced APs for the small and large WT and PLC$\delta4^{-/-}$ neurons. **P*<0.05; ****P*<0.001.

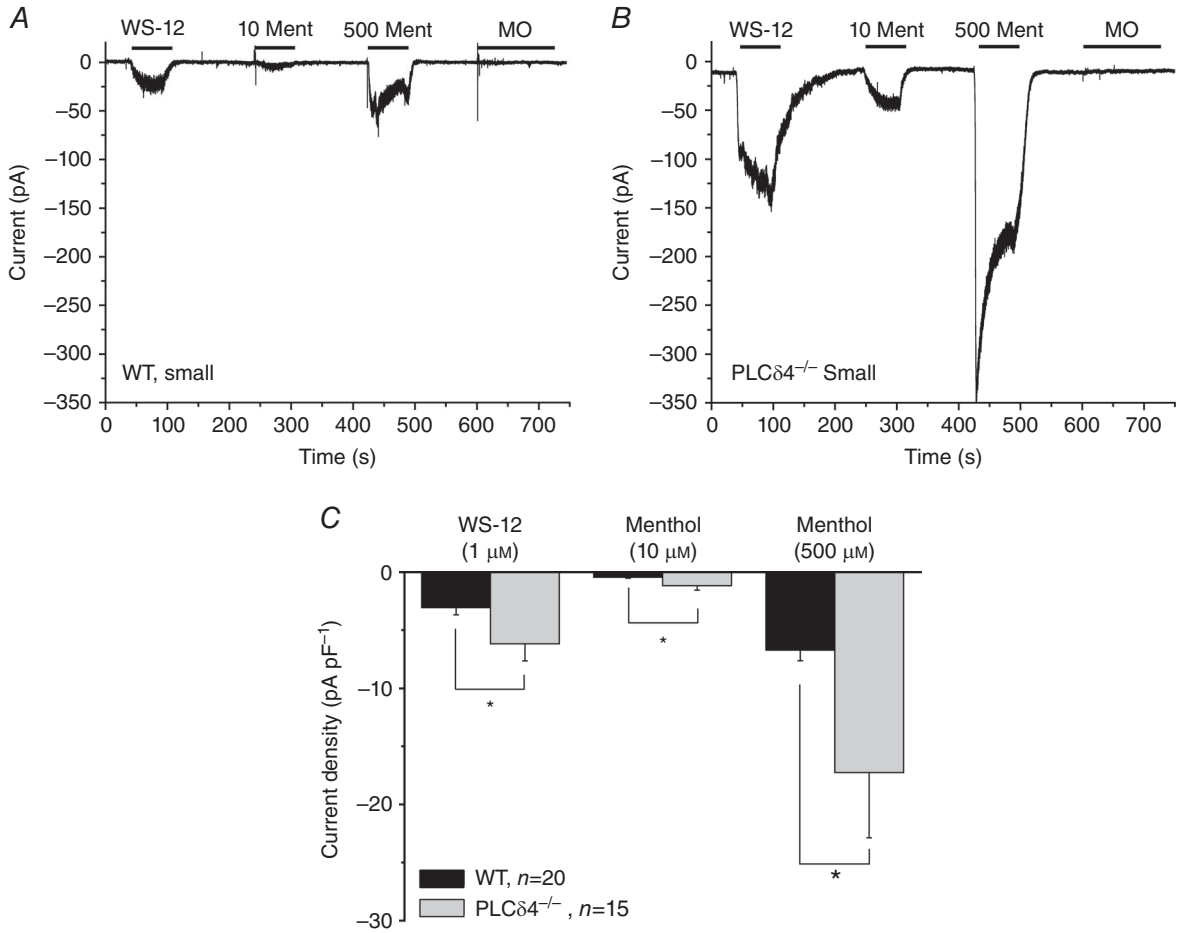

Figure 9. Inward currents induced by the selective TRPM8 agonist WS-12 in whole cell voltage-clamp experiments in small GFP-positive WT and PLC$\delta4^{-/-}$ DRG neurons
Experiments were performed as described in the Methods (V_h −60 mV). *A*, responses of a small GFP-positive WT neuron to 1 μM WS-12, 10 μM menthol, 500 μM menthol and 50 μM mustard oil (MO). *B*, similar experiment in a small GFP-positive PLC$\delta4^{-/-}$ neuron. C, data summary. **P*<0.05.

Heat and mechanical sensitivity is unaltered in PLC$\delta4^{-/-}$ mice

Our data so far show that TRPM8 activity is enhanced in PLC$\delta4^{-/-}$ mice, and that this translates to increased sensitivity to cold. PLC$\delta4^{-/-}$ small GFP-positive neurons, however, also showed increased responses to current injections, an effect probably independent of TRPM8. To test if the increased cold sensitivity in PLC$\delta4^{-/-}$ mice is part of an increased overall excitability, we tested mechanical and heat sensitivity of these mice. Figure 11*A* shows that paw withdrawal latency to radiant heat using the Hargreaves apparatus was not different between WT and PLC$\delta4^{-/-}$ mice. Similarly, there was no difference in the tail flick assay in response to hot water (48°C) (Fig. 11*B*). The sensitivity to mechanical stimuli using two different von Frey filaments (0.07 and 0.4 g) was not different from WT mice either (Fig. 11*C*, *D*).

Discussion

PLC isoforms in DRG neurons

The goal of this work was to establish the role of PLC in the regulation of cold sensitivity, and to identify the PLC isoform involved in the regulation of TRPM8 *in vivo*. There are 13 mammalian PLC isoforms (Fukami *et al.* 2010). PLCβ1–4 are activated by G-protein coupled receptors (GPCRs) and PLCγ1 and PLCγ2 are activated by receptor tyrosine kinases. While all PLC isoforms require some Ca^{2+} for activity, PLCδs, but not PLCβs or PLCγs, are thought to be activated by Ca^{2+} alone (Allen *et al.* 1997).

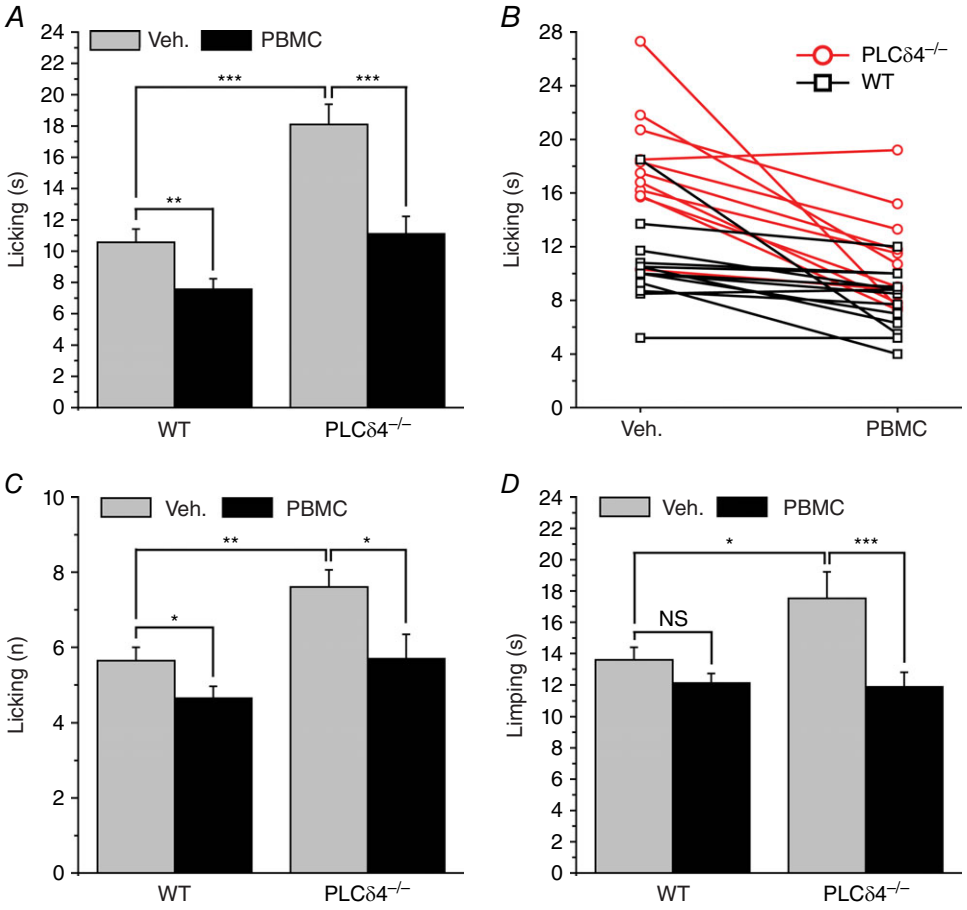

Figure 10. Higher cold sensitivity of PLC$\delta4^{-/-}$ mice in an evaporative cooling assay is inhibited by the TRPM8 antagonist PBMC
Behavioural responses such as number and duration of licking of the treated paw and of limping (dragging paw) in response to application of 50 μl acetone to the plantar surface of the hind paw were recorded as described in the Methods. *A*, duration of nocifensive events during the 5 min observation period are plotted in animals treated with vehicle or the TRPM8 antagonist PBMC (I.P., 10 mg kg^{-1}). *B*, individual duration of licking for WT and PLC$\delta4^{-/-}$ animals, and the responses to vehicle and PBMC. *C*, the number of nociceptive behavioural responses after the application of acetone. *D*, acetone application also induced changes from normal posture to limping on the treated paw, the duration of which is plotted. *P<0.05; **P<0.01, ***P<0.001; n = 11 for PLC$\delta4^{-/-}$ and n = 12 for WT animals.

The more recently discovered PLCη1 and 2 (Cockcroft, 2006), as well as the sperm-specific PLCζ, are also highly Ca^{2+} sensitive, but these isoforms are not expressed in DRG neurons (Lukacs *et al.* 2013; Thakur *et al.* 2014). PLCε RNA was found in whole DRGs, but was essentially absent from DRG neurons, suggesting predominantly glial expression (Thakur *et al.* 2014), and thus the most likely isoforms to be activated by Ca^{2+} influx in DRG neurons are PLCδs. We found earlier that PLCδ4 is expressed several fold higher in DRG neurons than the other two PLCδ isoforms PLCδ3 and PLCδ1 (Lukacs *et al.* 2013). These results were consistent with several high-throughput RNA sequencing studies (Hammer *et al.* 2010; Gerhold *et al.* 2013) including a recent one, where DRG neurons were separated from glial cells before RNA isolation (Thakur *et al.* 2014). PLCδ4 was also shown to be enriched in TRPM8-positive neurons (Knowlton *et al.* 2013), and thus this enzyme is a prime candidate for the PLC isoform activated by Ca^{2+} influx in DRG neurons and as a regulator of TRPM8 activity. The general phenotype of PLC$\delta4^{-/-}$ mice is quite moderate; apart from severely reduced male fertility, no other abnormalities have been reported (Fukami *et al.* 2001), so we used the existing global knockout mouse line to test the effect of the genetic deletion of this enzyme on TRPM8 activity in sensory neurons. We found that PLC$\delta4^{-/-}$ mice showed higher sensitivity to cold and TRPM8 agonists both in cellular electrophysiological assays and in behavioural experiments, showing the role of this enzyme in regulation of TRPM8 *in vivo*.

Difference between small and larger TRPM8-positive DRG neurons

One of our significant findings is that small and larger TRPM8-positive DRG neurons behave quite differently both in basic electrophysiological properties and in the difference between PLC$\delta4^{-/-}$ and WT mice. This is consistent with our earlier finding showing that small DRG neurons have higher menthol-induced current densities, and TRPM8 currents show higher levels of desensitization in these cells, compared to larger neurons (Yudin *et al.* 2011). PI(4,5)P_2 dialysed through the whole cell patch pipette also showed a stronger effect on desensitization in small neurons (Yudin *et al.* 2011), showing that PLC regulation of TRPM8 is primarily prevalent in small TRPM8-positive neurons. One possible explanation for the exclusive regulation in small neurons by PLCδ4 could be the much higher TRPM8 current densities in these neurons compared to larger cells. It is possible that the relatively low current densities in larger neurons do not generate a large enough Ca^{2+} influx to activate PLC.

An earlier study in rat DRG neurons also found that TRPM8 is expressed in both capsaicin-sensitive and

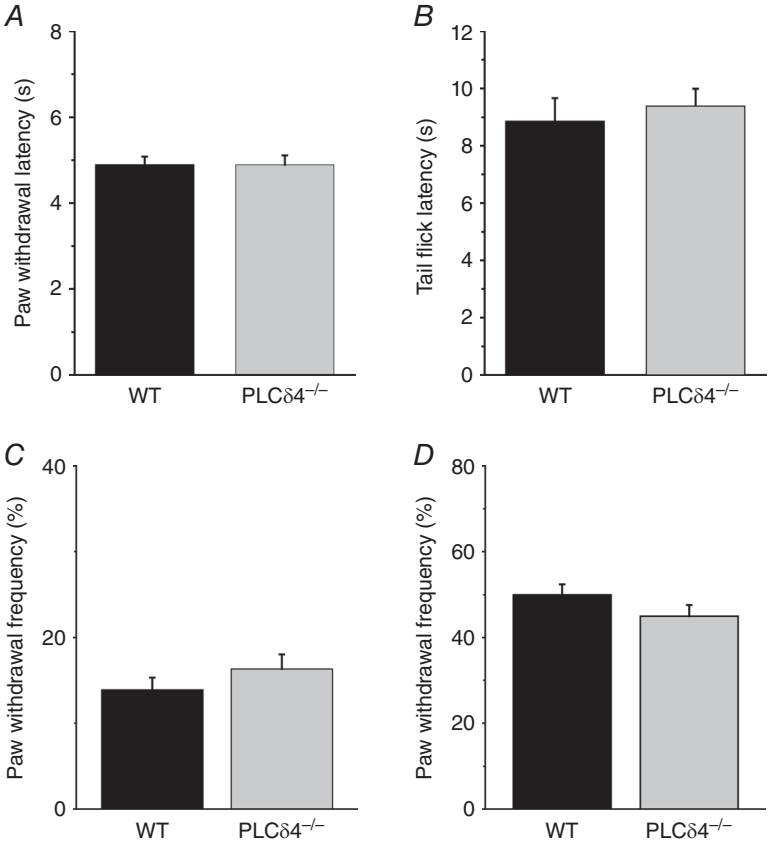

Figure 11. No difference in heat and mechanical sensitivity between WT and PLC$\delta4^{-/-}$ mice
Behavioural experiments using the Hargreaves apparatus, tail flick assay and von Frey assay were performed as described in the Methods. *A*, paw withdrawal latency in PLC$\delta4^{-/-}$ and WT mice in response to 52°C radiant heat (Hargreaves) ($n = 9$ for WT and $n = 15$ for PLC$\delta4^{-/-}$). *B*, responses of WT and PLC$\delta4^{-/-}$ mice to immersion of the tail into a water bath maintained at 48°C ($n = 9$ for WT and $n = 15$ for PLC$\delta4^{-/-}$). *C* and *D*, responses of WT and PLC$\delta4^{-/-}$ mice to von Frey filaments of 0.07 g (*C*) and 0.4 g (*D*) ($n = 9$ for WT and $n = 15$ for PLC$\delta4^{-/-}$).

capsaicin-insensitive neurons (Xing *et al.* 2006). The proportion of neurons responding to both capsaicin and cold increased in a rat chronic constrictive nerve injury model (Xing *et al.* 2007). Interestingly, in contrast to our data with mouse neurons, in rat DRG neurons cold- and menthol-induced responses were larger in capsaicin-insensitive neurons (Xing *et al.* 2006). Madrid *et al.* (2009) divided mouse cold-sensitive TG neurons into low threshold and high threshold neurons, and attributed the difference to differential expression of Kv1 channels and higher expression of TRPM8 in the low threshold neurons, but they found no size difference between the two subpopulations.

A recent study based on high throughput single cell RNA sequencing divided mouse DRG neurons into 11 groups using unbiased principal component analysis (Usoskin *et al.* 2015). Based on high menthol-induced current densities and responsiveness to capsaicin, small TRPM8-positive neurons from our work best fit the polymodal nociceptor group peptidergic PEP1 described in that study, in which both TRPM8 and TRPV1 RNA are enriched compared to other groups of neurons. It is less clear to what group, if any, the larger TRPM8-positive neurons described in our study correspond. There was no significant enrichment of PLCδ4 in the PEP1 group (Usoskin *et al.* 2015), and thus higher PLCδ4 expression in these cells is unlikely to account for the difference between small and larger neurons in our study.

Increased sensitivity of PLCδ4$^{-/-}$ mice to cold and TRPM8 agonists

We find that small PLCδ4$^{-/-}$ DRG neurons showed significantly higher responses to cold, menthol, and WS-12 compared to neurons from WT animals. Although there was a strong tendency ($P = 0.06$) for increased current desensitization in the first menthol application, the more marked and statistically significant difference was in the initial peak current amplitudes both for cold and for menthol. Our model for desensitization presumes a larger current decrease during continuous stimulation, rather than higher initial amplitudes. Why are initial current amplitudes higher in PLCδ4$^{-/-}$ neurons? We provide two lines of evidence that TRPM8 levels are not increased in PLCδ4$^{-/-}$ animals: current amplitudes evoked by a supramaximal stimulus were not different between PLCδ4$^{-/-}$ and WT animals, and we found no difference in TRPM8 protein levels in Western blot experiments.

One possible explanation for the higher initial peak amplitudes could be that due to some basal activity of TRPM8 and/or PLCδ4, some local PI(4,5)P_2 depletion had already occurred before cold or menthol application, leading to lower initial current amplitudes predominantly in WT neurons. An alternative explanation is the following. We use a relatively slow whole chamber perfusion, and thus it is possible that during the initial current increase, local PI(4,5)P_2 depletion already occurs before the current reaches its maximum. This could limit the level of the maximum current, and thus it is possible that the measured peaks reflect already partially desensitized currents to a higher extent in WT than in PLCδ4$^{-/-}$ neurons.

Our electrophysiology data show that the lack of PLCδ4 has a significant effect on TRPM8 channel activity in small TRPM8-positive neurons. PLCδ4$^{-/-}$ animals were also more sensitive to evaporative cold in behavioural experiments, showing that small neurons play an important role in this behavioural assay. Increased *in vivo* cold sensitivity is compatible with TRPM8 being more sensitive to cold, and especially that the TRPM8 antagonist had a stronger inhibitory effect in PLCδ4$^{-/-}$ mice than in control. Neuronal excitability, however, showed another, unexpected difference in PLCδ4$^{-/-}$ mice, a more sustained AP generation in response to depolarizations in small, but not larger GFP-positive neurons (Fig. 6*C*). This effect may also contribute to stronger responses to evaporative cold and also to higher AP frequency in response to menthol. While we did not pursue the mechanism of this effect, one potential explanation for the more sustained AP in response to current injections could be the following. We showed earlier that depolarization of DRG neurons by application of KCl also induced PLC activation and PI(4,5)P_2 depletion presumably because of the Ca^{2+} influx via voltage-gated Ca^{2+} channels (Lukacs *et al.* 2013). If some of the ion channels responsible for the AP generation are modulated by PI(4,5)P_2, the difference between the level of decrease in PI(4,5)P_2 between PLCδ4$^{-/-}$ and WT neurons may explain this phenomenon.

This TRPM8-independent increase in excitability, however, did not translate into increased sensitivity to heat and mechanical stimuli. The lack of effect of PLCδ4 deletion on heat sensitivity is intriguing, because most small TRPM8-positive neurons also expressed the heat- and capsaicin-sensitive TRPV1. TRPV1, similar to TRPM8, requires PI(4,5)P_2 for activity in a cellular environment (Rohacs, 2015), and depletion of this lipid by PLC activation upon Ca^{2+} influx plays a role in its desensitization (Lukacs *et al.* 2007). We have shown earlier that TRPV1 desensitization was moderately decreased in PLCδ4$^{-/-}$ mice (Lukacs *et al.* 2013). Deletion of TRPV1, however, had a clear effect on thermal hyperalgesia, but its effect on acute heat sensitivity is somewhat controversial (Caterina *et al.* 2000; Davis *et al.* 2000). The lack of effect of PLCδ4 deletion on heat sensitivity could also be due to higher apparent affinity of TRPV1 for PI(4,5)P_2 (Lukacs *et al.* 2007) compared to TRPM8 (Rohacs *et al.* 2005), which could make this channel less sensitive to small alterations in PI(4,5)P_2 levels than TRPM8.

While TRPM8 currents were higher in PLC$\delta4^{-/-}$ neurons than in control, they showed clear desensitization, arguing that PLC activation is still likely to occur despite the lack of PLCδ4. This could be due to the presence of the other two PLCδ isoforms, levels of which are slightly but not statistically significantly elevated in PLC$\delta4^{-/-}$ mice (Lukacs *et al.* 2013). Consistent with this notion, we find that co-expression of any of the three PLCδ isoforms accelerated desensitization of TRPM8, showing that the three different PLCδ isoforms are interchangeable in regulating TRPM8 activity. Alternatively, other Ca^{2+}-dependent pathways such as calmodulin (Sarria *et al.* 2011) or protein kinase C (Premkumar *et al.* 2005) may also contribute to desensitization.

DRG neurons express PLCβ isoforms, which are activated by GPCRs. Although PLCβ enzymes are not thought to be activated by Ca^{2+} alone, TRPM8 was proposed to have a GPCR-like activity, and was shown to induce depletion of $PI(4,5)P_2$ in TG neurons (Klasen *et al.* 2012). In contrast to PLCδs, however, co-expression of either PLCβ2 or PLCγ1 did not accelerate desensitization of TRPM8, arguing against significant involvement of PLCβs.

In conclusion, we identify PLCδ4 as a PLC isoform important in the regulation of TRPM8 both at the cellular level and *in vivo*.

References

Allen V, Swigart P, Cheung R, Cockcroft S & Katan M (1997). Regulation of inositol lipid-specific phospholipase Cδ by changes in Ca^{2+} ion concentrations. *Biochem J* **327**, 545–552.

Balla T (2001). Pharmacology of phosphoinositides, regulators of multiple cellular functions. *Curr Pharm Des* **7**, 475–507.

Bautista DM, Siemens J, Glazer JM, Tsuruda PR, Basbaum AI, Stucky CL, Jordt SE & Julius D (2007). The menthol receptor TRPM8 is the principal detector of environmental cold. *Nature* **448**, 204–208.

Bodding M, Wissenbach U & Flockerzi V (2007). Characterisation of TRPM8 as a pharmacophore receptor. *Cell Calcium* **42**, 618–628.

Brenner DS, Golden JP, Vogt SK, Dhaka A, Story GM & Gereau RW (2014). A dynamic set point for thermal adaptation requires phospholipase C-mediated regulation of TRPM8 *in vivo*. *Pain* **155**, 2124–2133.

Caterina MJ, Leffler A, Malmberg AB, Martin WJ, Trafton J, Petersen-Zeitz KR, Koltzenburg M, Basbaum AI & Julius D (2000). Impaired nociception and pain sensation in mice lacking the capsaicin receptor. *Science* **288**, 306–313.

Cockcroft S (2006). The latest phospholipase C, PLCζ, is implicated in neuronal function. *Trends Biochem Sci* **31**, 4–7.

Colburn RW, Lubin ML, Stone DJ, Jr, Wang Y, Lawrence D, D'Andrea MR, Brandt MR, Liu Y, Flores CM & Qin N (2007). Attenuated cold sensitivity in TRPM8 null mice. *Neuron* **54**, 379–386.

Daniels RL, Takashima Y & McKemy DD (2009). Activity of the neuronal cold sensor TRPM8 is regulated by phospholipase C via the phospholipid phosphoinositol 4,5-bisphosphate. *J Biol Chem* **284**, 1570–1582.

Davis JB, Gray J, Gunthorpe MJ, Hatcher JP, Davey PT, Overend P, Harries MH, Latcham J, Clapham C, Atkinson K, Hughes SA, Rance K, Grau E, Harper AJ, Pugh PL, Rogers DC, Bingham S, Randall A & Sheardown SA (2000). Vanilloid receptor-1 is essential for inflammatory thermal hyperalgesia. *Nature* **405**, 183–187.

Dhaka A, Murray AN, Mathur J, Earley TJ, Petrus MJ & Patapoutian A (2007). TRPM8 is required for cold sensation in mice. *Neuron* **54**, 371–378.

Fujita F, Uchida K, Takaishi M, Sokabe T & Tominaga M (2013). Ambient temperature affects the temperature threshold for TRPM8 activation through interaction of phosphatidylinositol 4,5-bisphosphate. *J Neurosci* **33**, 6154–6159.

Fukami K, Inanobe S, Kanemaru K & Nakamura Y (2010). Phospholipase C is a key enzyme regulating intracellular calcium and modulating the phosphoinositide balance. *Prog Lipid Res* **49**, 429–437.

Fukami K, Nakao K, Inoue T, Kataoka Y, Kurokawa M, Fissore RA, Nakamura K, Katsuki M, Mikoshiba K, Yoshida N & Takenawa T (2001). Requirement of phospholipase Cδ4 for the zona pellucida-induced acrosome reaction. *Science* **292**, 920–923.

Gerhold KA, Pellegrino M, Tsunozaki M, Morita T, Leitch DB, Tsuruda PR, Brem RB, Catania KC & Bautista DM (2013). The star-nosed mole reveals clues to the molecular basis of mammalian touch. *PLoS One* **8**, e55001.

Hammer P, Banck MS, Amberg R, Wang C, Petznick G, Luo S, Khrebtukova I, Schroth GP, Beyerlein P & Beutler AS (2010). mRNA-seq with agnostic splice site discovery for nervous system transcriptomics tested in chronic pain. *Genome Res* **20**, 847–860.

Horowitz LF, Hirdes W, Suh BC, Hilgemann DW, Mackie K & Hille B (2005). Phospholipase C in living cells: activation, inhibition, Ca^{2+} requirement, and regulation of M current. *J Gen Physiol* **126**, 243–262.

Karashima Y, Damann N, Prenen J, Talavera K, Segal A, Voets T & Nilius B (2007). Bimodal action of menthol on the transient receptor potential channel TRPA1. *J Neurosci* **27**, 9874–9884.

Klasen K, Hollatz D, Zielke S, Gisselmann G, Hatt H & Wetzel CH (2012). The TRPM8 ion channel comprises direct Gq protein-activating capacity. *Pflugers Arch* **463**, 779–797.

Knowlton WM, Daniels RL, Palkar R, McCoy DD & McKemy DD (2011). Pharmacological blockade of TRPM8 ion channels alters cold and cold pain responses in mice. *PLoS One* **6**, e25894.

Knowlton WM, Palkar R, Lippoldt EK, McCoy DD, Baluch F, Chen J & McKemy DD (2013). A sensory-labeled line for cold: TRPM8-expressing sensory neurons define the cellular basis for cold, cold pain, and cooling-mediated analgesia. *J Neurosci* **33**, 2837–2848.

Liu B, Fan L, Balakrishna S, Sui A, Morris JB & Jordt SE (2013). TRPM8 is the principal mediator of menthol-induced analgesia of acute and inflammatory pain. *Pain* **154**, 2169–2177.

Liu B & Qin F (2005). Functional control of cold- and menthol-sensitive TRPM8 ion channels by phosphatidylinositol 4,5-bisphosphate. *J Neurosci* **25**, 1674–1681.

Lukacs V, Thyagarajan B, Varnai P, Balla A, Balla T & Rohacs T (2007). Dual regulation of TRPV1 by phosphoinositides. *J Neurosci* **27**, 7070–7080.

Lukacs V, Yudin Y, Hammond GR, Sharma E, Fukami K & Rohacs T (2013). Distinctive changes in plasma membrane phosphoinositides underlie differential regulation of TRPV1 in nociceptive neurons. *J Neurosci* **33**, 11451–11463.

Madrid R, de la Pena E, Donovan-Rodriguez T, Belmonte C & Viana F (2009). Variable threshold of trigeminal cold-thermosensitive neurons is determined by a balance between TRPM8 and Kv1 potassium channels. *J Neurosci* **29**, 3120–3131.

Malin SA, Davis BM & Molliver DC (2007). Production of dissociated sensory neuron cultures and considerations for their use in studying neuronal function and plasticity. *Nat Protoc* **2**, 152–160.

McKemy DD, Neuhausser WM & Julius D (2002). Identification of a cold receptor reveals a general role for TRP channels in thermosensation. *Nature* **416**, 52–58.

Orio P, Madrid R, de la Pena E, Parra A, Meseguer V, Bayliss DA, Belmonte C & Viana F (2009). Characteristics and physiological role of hyperpolarization activated currents in mouse cold thermoreceptors. *J Physiol* **587**, 1961–1976.

Peier AM, Moqrich A, Hergarden AC, Reeve AJ, Andersson DA, Story GM, Earley TJ, Dragoni I, McIntyre P, Bevan S & Patapoutian A (2002). A TRP channel that senses cold stimuli and menthol. *Cell* **108**, 705–715.

Premkumar LS, Raisinghani M, Pingle SC, Long C & Pimentel F (2005). Downregulation of transient receptor potential melastatin 8 by protein kinase C-mediated dephosphorylation. *J Neurosci* **25**, 11322–11329.

Rohacs T (2014). Phosphoinositide regulation of TRP channels. *Handb Exp Pharmacol* **233**, 1143–1176.

Rohacs T (2015). Phosphoinositide regulation of TRPV1 revisited. *Pflugers Arch* **467**, 1851–1869.

Rohacs T, Lopes CM, Michailidis I & Logothetis DE (2005). $PI(4,5)P_2$ regulates the activation and desensitization of TRPM8 channels through the TRP domain. *Nat Neurosci* **8**, 626–634.

Sarria I, Ling J, Zhu MX & Gu JG (2011). TRPM8 acute desensitization is mediated by calmodulin and requires PIP_2: distinction from tachyphylaxis. *J Neurophysiol* **106**, 3056–3066.

Sherkheli MA, Gisselmann G, Vogt-Eisele AK, Doerner JF & Hatt H (2008). Menthol derivative WS-12 selectively activates transient receptor potential melastatin-8 (TRPM8) ion channels. *Pak J Pharm Sci* **21**, 370–378.

Story GM, Peier AM, Reeve AJ, Eid SR, Mosbacher J, Hricik TR, Earley TJ, Hergarden AC, Andersson DA, Hwang SW, McIntyre P, Jegla T, Bevan S & Patapoutian A (2003). ANKTM1, a TRP-like channel expressed in nociceptive neurons, is activated by cold temperatures. *Cell* **112**, 819–829.

Takashima Y, Daniels RL, Knowlton W, Teng J, Liman ER & McKemy DD (2007). Diversity in the neural circuitry of cold sensing revealed by genetic axonal labeling of transient receptor potential melastatin 8 neurons. *J Neurosci* **27**, 14147–14157.

Thakur M, Crow M, Richards N, Davey GI, Levine E, Kelleher JH, Agley CC, Denk F, Harridge SD & McMahon SB (2014). Defining the nociceptor transcriptome. *Front Mol Neurosci* **7**, 87.

Usoskin D, Furlan A, Islam S, Abdo H, Lonnerberg P, Lou D, Hjerling-Leffler J, Haeggstrom J, Kharchenko O, Kharchenko PV, Linnarsson S & Ernfors P (2015). Unbiased classification of sensory neuron types by large-scale single-cell RNA sequencing. *Nat Neurosci* **18**, 145–153.

Varnai P, Thyagarajan B, Rohacs T & Balla T (2006). Rapidly inducible changes in phosphatidylinositol 4,5-bisphosphate levels influence multiple regulatory functions of the lipid in intact living cells. *J Cell Biol* **175**, 377–382.

Viana F, de la Pena E & Belmonte C (2002). Specificity of cold thermotransduction is determined by differential ionic channel expression. *Nat Neurosci* **5**, 254–260.

Wu ZZ & Pan HL (2007). Role of TRPV1 and intracellular Ca^{2+} in excitation of cardiac sensory neurons by bradykinin. *Am J Physiol Regul Integr Comp Physiol* **293**, R276–283.

Xing H, Chen M, Ling J, Tan W & Gu JG (2007). TRPM8 mechanism of cold allodynia after chronic nerve injury. *J Neurosci* **27**, 13680–13690.

Xing H, Ling J, Chen M & Gu JG (2006). Chemical and cold sensitivity of two distinct populations of TRPM8-expressing somatosensory neurons. *J Neurophysiol* **95**, 1221–1230.

Yudin Y, Lukacs V, Cao C & Rohacs T (2011). Decrease in phosphatidylinositol 4,5-bisphosphate levels mediates desensitization of the cold sensor TRPM8 channels. *J Physiol* **589**, 6007–6027.

Yudin Y & Rohacs T (2011). Regulation of TRPM8 channel activity. *Mol Cell Endocrinol* **353**, 68–74.

Zakharian E, Cao C & Rohacs T (2010). Gating of transient receptor potential melastatin 8 (TRPM8) channels activated by cold and chemical agonists in planar lipid bilayers. *J Neurosci* **30**, 12526–12534.

Zhao X, Tang Z, Zhang H, Atianjoh FE, Zhao JY, Liang L, Wang W, Guan X, Kao SC, Tiwari V, Gao YJ, Hoffman PN, Cui H, Li M, Dong X & Tao YX (2013). A long noncoding RNA contributes to neuropathic pain by silencing Kcna2 in primary afferent neurons. *Nat Neurosci* **16**, 1024–1031.

Additional information

Competing interests

The authors declare no conflict of interest.

Author contributions

T.R. and Y.Y. conceived and designed the experiments. Y.Y. performed the electrophysiology experiments on DRG neurons,

the acetone test and the tail flick assay, B.L. performed the Hargreaves test and the von Frey test, T.R. performed the *Xenopus* oocyte experiments. Y.Y., B.L., Y.X.T. and T.R. analysed and interpreted the data. The experiments were performed at the Department of Pharmacology, Physiology and Neuroscience, and at the Department of Anesthesiology at Rutgers New Jersey Medical School. T.R. and Y.Y. wrote the paper, Y.Y., Y.X.T., B.L. and T.R. critically reviewed the manuscript. All authors have approved the final version of the manuscript and agree to be accountable for all aspects of the work. All persons designated as authors qualify for authorship, and all those who qualify for authorship are listed.

Funding

This work was supported by NIH grants R01NS055159 and R01GM093290 to T.R., and F31NS092310 to B.L.

Acknowledgements

The TRPM8-GFP mouse line was generously provided by Dr David McKemy (University of Southern California), and the PLCD4$^{-/-}$ line by Dr Kiyoko Fukami (Tokyo University). The help of Ms Luyu Liu with the behavioural experiments is highly appreciated. The help of Dr Viktor Lukacs with oocyte experiments at early stages of this project is also appreciated.